



Molecular characterization of a cDNA encoding $\text{Na}^+/\text{K}^+/\text{2Cl}^-$ cotransporter in the gill of mud crab (*Scylla paramamosain*) during the molt cycle: Implication of its function in osmoregulation

Bin-peng Xu^a, Dan-dan Tu^a, Mao-cang Yan^b, Miao-an Shu^{a,*}, Qing-jun Shao^a

^a College of Animal Sciences, Zhejiang University, Hangzhou 310058, Zhejiang Province, China

^b Zhejiang Mariculture Research Institute, Wenzhou 325005, Zhejiang Province, China

ARTICLE INFO

Article history:

Received 20 February 2016

Received in revised form 19 August 2016

Accepted 19 August 2016

Available online 1 September 2016

Keywords:

Decapod crustaceans

Gill structure

Hemolymph

Ion transporters

Molt

Ionoregulation

ABSTRACT

Although iono-regulatory processes are critical for survival of crustaceans during the molt cycle, the mechanisms involved are still not clear. The $\text{Na}^+/\text{K}^+/\text{2Cl}^-$ cotransporter (NKCC), a SLC12A family protein that transports Na^+ , K^+ and 2Cl^- into cells, is essential for cell ionic and osmotic regulation. To better understand the role of NKCC in the molt osmoregulation, we cloned and characterized a NKCC gene from the mud crab, *Scylla paramamosain* (designated as *SpNKCC*). The predicted *SpNKCC* protein is well conserved, and phylogenetic analysis revealed that this protein was clustered with crustacean NKCC. Expression of *SpNKCC* was detected in all the tissues examined but was highest in the posterior gills. Transmission electron microscopy revealed that posterior gills had a thick type of epithelium for ion regulation while the anterior gills possessed a thin phenotype related to gas exchange. During the molting cycle, hemolymph osmolality and ion concentrations (Na^+ and Cl^-) increased significantly over the postmolt period, remained stable in the intermolt and premolt stages and then decreased at ecdysis. Meanwhile, the expression of *SpNKCC* mRNA was significantly elevated (26.7 to 338.8-fold) at the ion re-establishing stages (postmolt) as compared with baseline molt level. This pattern was consistent with the coordinated regulation of Na^+/K^+ -ATPase α -subunit (*NKA α*), carbonic anhydrase cytoplasmic (*CAC*) isoform and Na^+/H^+ exchanger (*NHE*) genes in the posterior gills. These data suggest that *SpNKCC* may be important in mediating branchial ion uptake during the molt cycle, especially at the postmolt stages.

© 2016 Elsevier Inc. All rights reserved.

Introduction

Molting, a phenomenon of the periodic shedding the old cuticle and subsequent reconstruction of a new rigid exoskeleton, occurs in all crustaceans and is essential for growth, metamorphosis and reproduction (Ghanawi and Saoud, 2012; Li et al., 2015). Generally, the molt cycle in decapod crustaceans is composed of different stages, including preecdysis (pre-molt, D stage), ecdysis (E stage), postecdysis (postmolt, A and B stages) and intermolt (C stage) stages (Drach and Tchernigovtzeff, 1967). At ecdysis, the shedding of the restrictive cuticle and the size increase in crustaceans are achieved by the enhanced water absorption (Perry et al., 2001; Wilder et al., 2009). Such increase in water uptake may lead to a simultaneous decrease in hemolymph osmolality and ion concentrations in crustaceans. Hence, osmoregulation is directly affected by the molting process.

Crustaceans do have to keep hemolymph osmolality and major ionic concentrations (Na^+ , Cl^-) within the range of physiological homeostasis

through absorption and excretion of Na^+ and Cl^- across the gills (, which produce

H^+ and HCO_3^- needed to support Na^+/H^+ and $\text{HCO}_3^-/\text{Cl}^-$ exchange, respectively (Henry, 1988; Serrano and Henry, 2008; McNamara and Faria, 2012). Studies have indicated that $\text{Na}^+/\text{K}^+/\text{2Cl}^-$ cotransporter (NKCC) may also serve as a key ion transporter for marine invertebrates (Riestenpatt et al., 1996; Luquet et al., 2005; Havird et al., 2014).

The $\text{Na}^+/\text{K}^+/\text{2Cl}^-$ cotransporter (NKCC), is a member of the cation-chloride cotransporter (CCC) family that plays an essential role in the osmoregulatory processes in the gills of aquatic species by transporting Na^+ , K^+ and Cl^- into animal cells simultaneously (Gagnon et al., 2002; Gamba, 2005). In vertebrates, two distinct isoforms of NKCC cotransporters (NKCC1 and NKCC2) have been identified (Markadieu

* Corresponding author at: Animal Sciences College, Zhejiang University, Zijingang Campus, 866 Yuhangtang Road, Hangzhou 310058, China.
E-mail address: shuma@zju.edu.cn (M. Shu).

2.1. Animal collection and maintenance

The experimental animals, *Scylla paramamosain*, measuring 40.05 ± 6.87 g in weight, were obtained from Wenzhou, Zhejiang Province, China. All individuals were cultured individually in plastic trays ($0.3 \times 0.2 \times 0.2$ m) with running seawater of approximately 17 ppt salinity as their original culture water at 29 ± 1 °C. Crabs were fed with live clams every day until 2 days before sampling.

The molt stages were determined by observing the setae on the maxilliped exopodite on the animals under a light microscope (Xu et al., 2015). A and B stages were designated as postmolt stages, C as intermolt, D₀ as early premolt, D₁ as mid premolt, D₂ as late premolt, and E as ecdysis, based on the established criteria (Drach and Tchernigovtzeff, 1967).

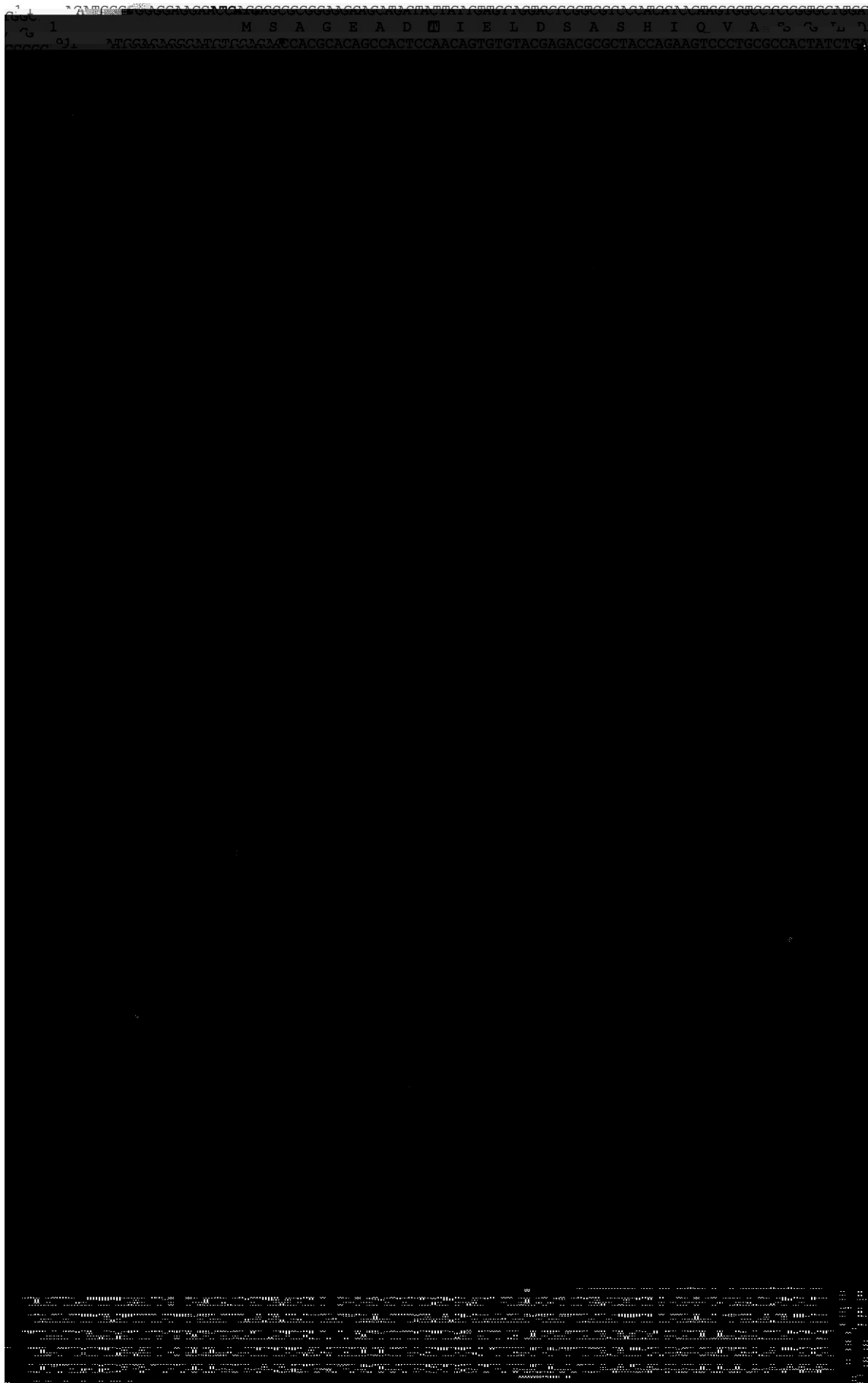
2.2. Tissue preparation

Crabs ($n = 7$) in each stage of the molt cycle were sampled. Briefly, hemolymph samples were withdrawn from the infrabranial sinus at the base of the fifth pereopod using a 22-gauge needle and 1 mL syringe. The samples were frozen at -20 °C until osmolality determination and ion analysis. For dissection, crabs were anesthetized on crushed ice for 10 min and then anterior (G1), posterior (G6) gills and other tissues (gills, muscle, hepatopancreas, gut, thoracic ganglia, hypodermis, hemocytes, antennal gland and heart) were dissected out and immediately placed in liquid nitrogen and kept at -80 °C until required. Only specimens in the intermolt stage were used for tissue distribution analysis, histological and electron microscopic study.

2.3. Growth metrics

The quantitative method was used as previously described (Chang et al., 2011). At the beginning of the study, crabs ($n = 7$) from the late premolt stage D₂ were selected and measured individually for carapace parameters (width and length) and weight to the nearest 0.1 mm and 0.01 g, respectively. The crabs were held as described above and the general molting state of these crabs was observed frequently. After ecdysis, carapace param15.46(l)23.22(w)189.1(w)14.e(e)15(r)14.8(e)-184.1(m)

and Delpire, 2014). In contrast, a unique NKCC has been identified from crustaceans, including *Callinectes sapidus* (Towle et al., 1997b), *Carcinus maenas*, *Chasmagnathus granulatus* (Luquet et al., 2005) and *Halocaridina rubra* (Havird et al., 2014). NKCC exhibits a salinity-sensitive expression pattern, and its transcription level increases when crustaceans are exposed to low salinity water (Spanings-Pierrot and Towle, 2004; Luquet et al., 2005; Havird et al., 2014). The NKCC was presumably involved in the initial step of ion transport from the ambient medium to the gill. In the green shore crab *C. maenas*, electrophysiological evidence has been presented for the participation of an apical NKCC in this process (Riestenpatt et al., 1996). Although there is a growing number of evidence implicating the involvement of crustacean NKCC activity in ionic homeostasis in different salinities, very little is known about whether NKCC is involved in osmoregulation during the molt processes in crustaceans. Therefore, the aim of the present study was to gain new insights into the characterization of NKCC and its role in osmoregulation in different molt stages of mud crab (*Scylla paramamosain*), a euryhaline species that was found to molt at least 18 times after metamorphosis (Ong, 1966; Chung and Lin, 2006). Here, we report the molecular cloning of a NKCC from gills of *S. paramamosain*. Further, hemolymph osmolality, ion concentration as well as the mRNA expression patterns of NKCC, Na⁺/K⁺-ATPase α -subunit (*NKA* α), carbonic anhydrase cytoplasmic (*CAC*) isoform, *NHE* and aquaporin-1 (*AQP-1*) in the gills of various molt stages were determined. In addition, gill architecture of the intermolt animals has also been studied to assess its possible role as a site for osmoregulation. These findings are brought together to elucidate the biochemical, transcriptional and ultrastructural underpinnings of ion regulation in crustacean during the molt cycle.



2.5. Cloning and sequencing of the branchial NKCC

2.5.1. cDNA fragments amplification

Total RNA was extracted from gills of *S. paramamosain* by using RNAiso Plus (TaKaRa, Dalian, China) according to the manufacturer's protocol. All RNA samples treated with gDNA Eraser were subjected to syntheses of cDNAs using PrimeScript® RT reagent Kit (TaKaRa, Dalian, China).

To obtain the cDNA fragment of *SpNKCC* (*S. paramamosain* NKCC), degenerate primers *SpNKCC-F* and *SpNKCC-R* (Table 1) were designed based on the homologies between published NKCC sequences. PCR for putative *SpNKCC* segments were performed and the PCR products were electrophoresed on an agarose gel, purified and cloned into a pMD19-T vector with a TA cloning kit (TaKaRa, Dalian, China). The recombinant plasmids were transformed into DH5 α chemically competent cell of *Escherichia coli* (TaKaRa, Dalian, China). The positive clones were screened by PCR and then sequenced. Finally, the resulting sequences were verified and subjected to analysis in NCBI.

2.5.2. Rapid amplification of cDNA ends (RACE)

To synthesize first-strand cDNA for RACE reactions, 1 μ g mRNA was reverse transcribed using reagents and a protocol provided in a SMARTer™ RACE cDNA Amplification Kit (Clontech, Palo Alto, CA, USA). Both the 3'-cDNA end and the 5'-cDNA end reaction conditions and components were performed according to the manufacturer's instructions. PCR products were isolated, purified, cloned, and sequenced as described in the cDNA fragment amplification. Primers were listed in Table 1.

2.6. Bioinformatics analysis

The full-length cDNA sequence was identified by BLAST analysis in NCBI database (<http://www.ncbi.nlm.nih.gov>). The predicted amino acid sequence was determined using the EXPASY molecular biology server (<http://web.expasy.org/blast/>). *SpNKCC* molecular mass and phosphorylation sites were predicted by ProtParam (<http://web.expasy.org/protparam/>) and NetPhos programs (<http://www.cbs.dtu.dk/services/NetPhos/>), respectively. Prediction of NKCC domain and features were performed using the InterPro Scan (<http://www.ebi.ac.uk/interpro/scan.html>). N-glycosylation sites were predicted at (<http://www.cbs.dtu.dk/services/NetNGlyc/>). Multiple alignments were performed using the ClustalX 1.81 software (<http://www.clustal.org/>) and edited by the GeneDoc software (<http://www.psc.edu/biomed/genedoc/>). The neighbor-joining tree estimated from distances between the animal NKCC amino acid sequences was built by Mega version 5.0 (<http://www.megasoftware.net/>), using P-distance and 1000 bootstrap (Tamura et al., 2011). Deduced protein sequences of NKCC from various species were retrieved from the GenBank (<http://www.ncbi.nlm.nih.gov/genbank/>).

2.7. Tissue distribution

Total RNA from the different tissues (gills, muscle, hepatopancreas, gut, thoracic ganglia, hypodermis, hemocytes, antennal gland and heart) of crabs (intermolt) was isolated to investigate the tissue distribution of *SpNKCC*. After cDNA was synthesized, quantitative real-time polymerase chain reaction (qPCR) were assayed for the levels of *SpNKCC* expression using an SYBR® Advantage® qPCR Premix (TaKaRa, Dalian, China) on an Applied Biosystems 7500 instrument (Applied Biosystems Carlsbad, CA).

SpNKCC real-F and *SpNKCC* real-R were used to generate *SpNKCC* fragment, while β -actin real-F and β -actin real-R were used to amplify corresponding β -actin fragment as the reference (Chung and Lin, 2006; Huang et al., 2012). All primers for the qPCR were ensured to produce a single PCR product of the predicted size and were quantified using the standard curve generated from serial dilutions (1, 0.1, 0.01, 0.001 and 0.0001 fold dilution series) of cDNA transcribed from gills mRNA. The real time PCR reaction was performed in triplicates in a final volume of 20 μ L reaction mixture each (10 μ L of SYBR Premix Ex Taq, 6.8 μ L of water, 2 μ L of cDNA, 0.4 μ L of ROX and 0.4 μ L of each primer). PCR conditions were as follows: 95 °C for 30 s; 40 cycles at 95 °C for 5 s and 60 °C for 30 s; and a melt from 60 to 95 °C. The relative expression level of *SpNKCC* was calculated by the comparative threshold cycle method ($2^{-\Delta\Delta Ct}$) (Livak and Schmittgen, 2001).

2.8. Histological and electron microscopic study

The anterior gills (Gills 1) and posterior gills (Gills 6) were dissected from 3 animals in intermolt stage. For the histology analysis, gills were incubated in 10% formaldehyde solution for 48 h, dehydrated in graded alcohol series, cleared with xylene and embedded in paraffin. Tissue sections (4 μ m) were stained with hematoxylin–eosin (H&E) for general morphology and observed under a microscope (Nikon, Tokyo, Japan). Pictures were taken with 400 \times magnification using a microscope digital camera (Toupcam, Hangzhou, China).

For transmission electron microscopy (TEM) study, specimens were fixed with 2.5% glutaraldehyde overnight. Fol016.8(b35.9(tv)-13.c0TD(ca)3

2.11. Statistical analysis

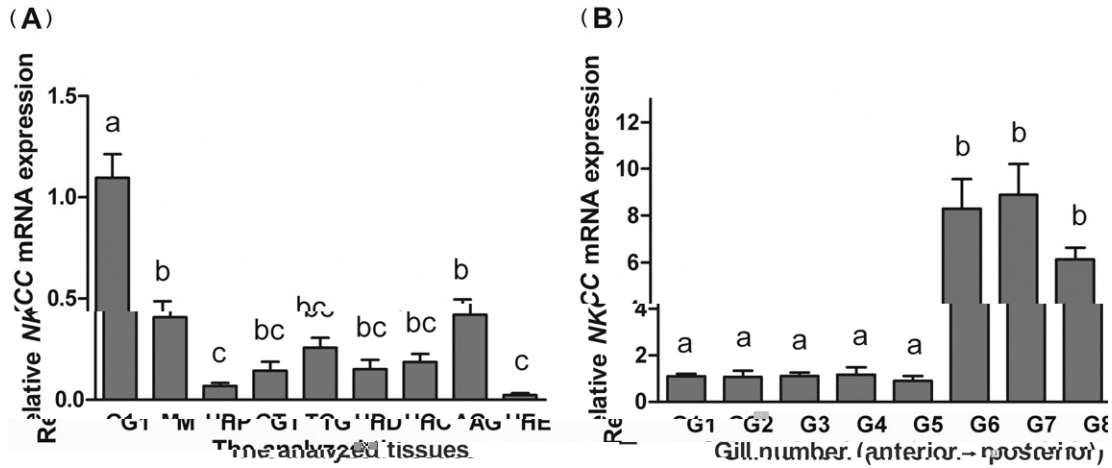
The data were subjected to statistical analysis by a one-way ANOVA followed by Tukey's multiple comparisons or unpaired Student *t*-test when appropriate using Prism 5.0 (Graph-Pad, La Jolla, CA). The observed differences were considered significant at $P < 0.05$. All data were presented as means \pm standard error (SEM) of triplicate measurements on each of seven separate preparations.



3.1. cDNA cloning and sequence analysis of SpNKCC

A full-length cDNA (4151 base pairs) corresponding to a NKCC gene of *Scylla paramamosain* (GenBank accession no. _____) was obtained by RT-PCR coupled to RACE-PCR. The nucleotide and deduced amino acid sequence are shown in Fig. 1. The corresponding gene was designated as SpNKCC. It is composed of a 15-bp 5'-untranslated region (UTR), a 3162-bp open reading frame (ORF) and a 974-bp 3'-UTR. The open reading frame encodes a 1053 amino acid protein. A GT-repeat motif is located 824 bp upstream of the polyadenylation signal (AATA AA) in the 3'-UTR region (Fig. 1). The deduced protein has a predicted molecular mass of about 116.5 kDa and a theoretical pI of 6.08. It consists of a SLC12A domain (residues 117-631) of 414 amino acid residues followed by 12 transmembrane domains and a hydrophilic cytoplasmic C-terminal tail (residues 640-1053) (Fig. 1). In addition, the protein has 8 putative N-linked glycosylation sites (Fig. 2, bold N at positions 237, 396, 407, 416, 529, 653, 781 and 1044) and 51 potential phosphorylation sites (31 serine, 12 threonine and 8 tyrosine), respectively (Fig. 1).

Multiple protein sequence alignment analysis is shown in Fig. 2. Although the similarity of this gene was low compared to vertebrates NKCCs (63.70%–65.88%), the SpNKCC revealed high similarity to other decapoda NKCC from crustaceans (87.28%–97.22%). A phylogenetic analysis of the NKCC protein sequences revealed the expected relationship between *S. paramamosain* and other species (Fig. 3). Accordingly, NKCCs can be divided into two subclasses: vertebrate NKCCs (NKCC1 and NKCC2) and invertebrate NKCC. In the invertebrates, SpNKCC was clustered with blue crab NKCC -/11Tf1.5009-225.838(G)27.tns(m)-293.esbat2



Expression of *SpNKCC* in the tissues obtained from juvenile crabs at intermolt stage. The tissue distribution of *SpNKCC* in crab is shown relative to expression in gill 1. (A) *SpNKCC* transcript levels in crab tissues: G1 = gill 1, M = muscle, HP = hepatopancreas, GT = gut, TG = thoracic ganglion, HD = hypodermis, HC = hemocytes, AG = antennal gland and HE = heart. (B) Expression of *SpNKCC* in gills 1–8. G1–G8, individual gills from the anterior to the posterior of the crab. Vertical bars represent the mean \pm SEM, $n = 7$. Means with different superscript letters are significantly different (one-way ANOVA, Tukey's multiple comparisons test, $P < 0.05$).

the carapace length was increased from 34.1 ± 0.2 mm to 42.5 ± 0.1 mm (Student's *t*-test, $P < 0.05$, Fig. 7A), respectively.

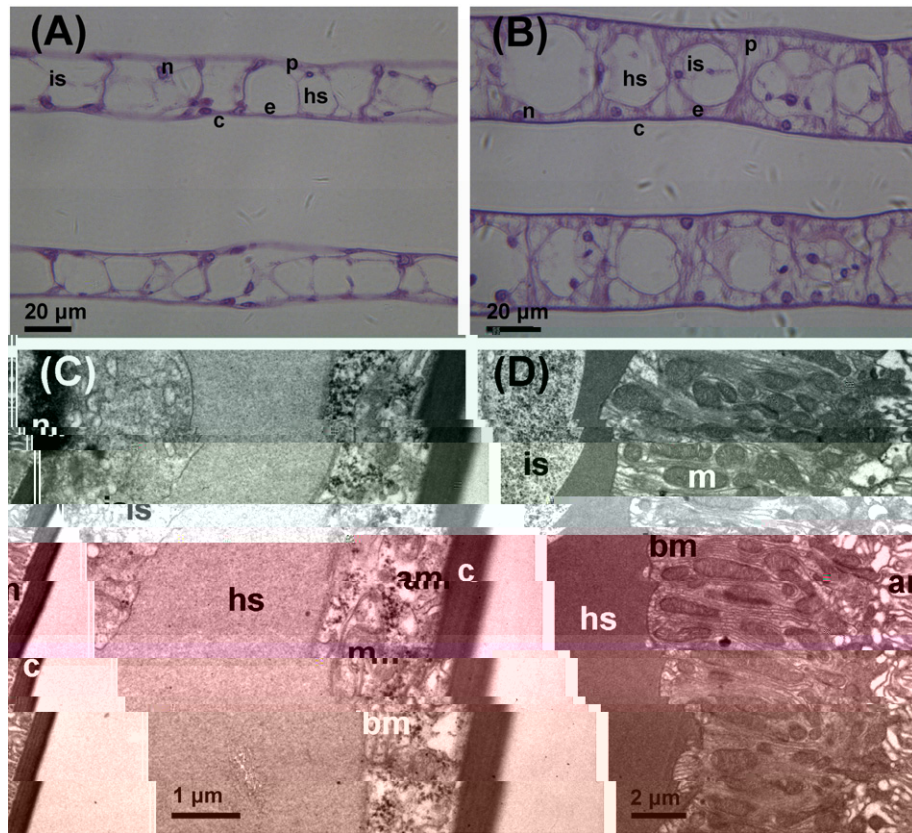
3.6. Expression of *SpNKCC* in posterior gills during molt cycle

To gain some insight into the potential role of *SpNKCC* during the molt cycle, the expression level of its gene was quantified by qPCR in posterior gills at various molt stages (Fig. 8). The expression was lowest in molt (used as calibrator). This transcript then attained a high expression level

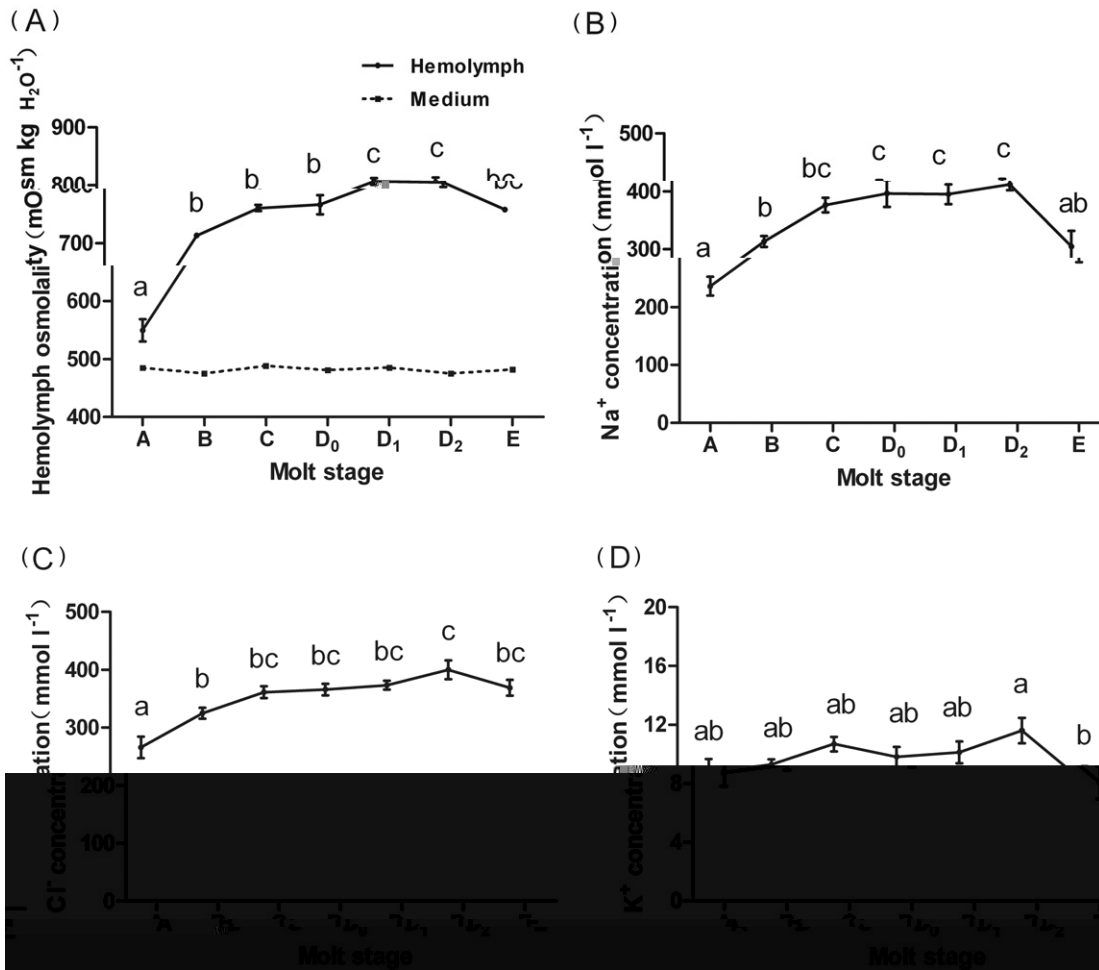
at early premolt (stage A, 26.7-fold, ANOVA, $P < 0.05$). It significantly elevated at late premolt (stage B, 338.8-fold, ANOVA, $P < 0.05$) and then decreased during the following intermolt and premolt stages (stage C–D₂).

3.7. Branchial gene expression of *NKA α*, *NHE*, *CAC* and *AQP-1* during the molt cycle

To characterize differences in iono-regulatory mechanisms in the posterior gills of *S. paramamosain* at different molt stages, we examined



Structures of epithelial cells in posterior (A–C) and anterior gill (B–D) of *S. paramamosain* (intermolt). Photomicrographs of semi-thin sections of gill 1 (A) and 6 (B) lamellae stained with hematoxylin-eosin (H & E). Both images are 400 \times . (C) Ultrastructure of respiratory-type cell in anterior gill epithelium of the *S. paramamosain*. (D) Ultrastructure of ion-transporting-type cell in posterior gill epithelium of the *S. paramamosain*. am: apical membrane; bm: basal membrane; c: cuticle; e: epithelial cell; hs: hemolymph space; is: intralamellar septum; m: mitochondrion; n: nucleus; p: pillar cell. Scale bar in (A) and (B), 20 μ m; in (C), 1 μ m and (D), 2 μ m.



gene expression of key ion transporting proteins and water channel previously characterized in other euryhaline crabs (Fig. 9). Homologs of *NHE*, *CAC* (osmoregulatory isoform) and *AQP-1* were identified from the *S. paramamosain* gills (Supplementary File 2), and GenBank accession numbers are _____, _____ and _____, respectively.

The patterns of expression of mRNA abundance for the *NKA α* (Fig. 9A), *CAC* and *NHE* were similar to that for *NKCC*. Following ecdysis, *NKA α* mRNA in posterior gills increased 9.5-fold at stage A over the level in animals at stage E (ANOVA, $P < 0.05$), and elevated at stage B (41.7-fold, ANOVA, $P < 0.05$), then fell sharply at intermolt and premolt (ANOVA, $P < 0.05$). In posterior gills, the level of *CAC* transcript (Fig. 9B) was lowest in molting crabs, and it increased about 21.4-fold to a peak in postmolt stage B (ANOVA, $P < 0.05$). It was then gradually decreased to the similar level of that at stage A (ANOVA, $P < 0.05$). Similarly, *NHE* transcription in posterior gills (Fig. 9C) was significantly raised in the postmolt stage B (79.9-fold, ANOVA, $P < 0.05$), then followed by a decreasing trend from intermolt to premolt.

The pattern of *AQP-1* mRNA expression over the molt cycle was, however, different from that of *NKCC* gene expression (Fig. 9D). The expression level of *AQP-1* mRNA in posterior gills was low during the intermolt and premolt and then increased 3.8-fold at the molting stage E (ANOVA, $P < 0.05$), and remained high during the postmolt (stage A–B).

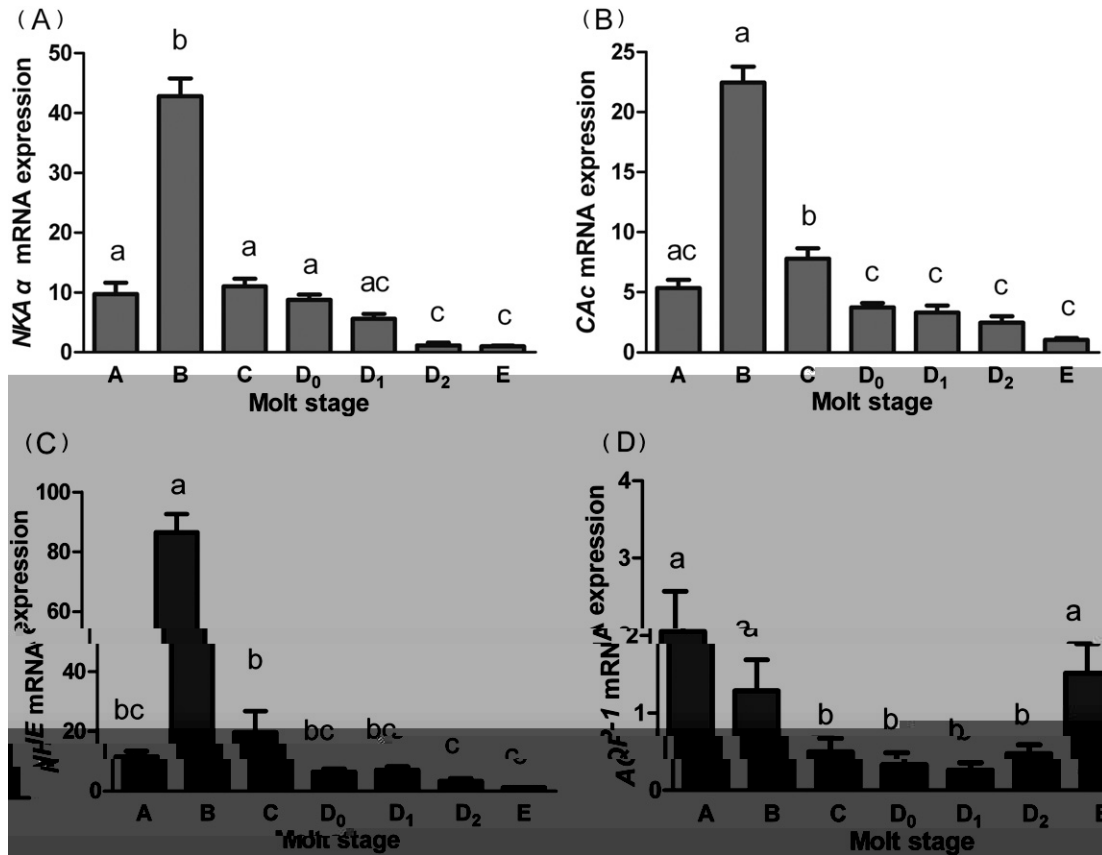
Data presented in the current study provide the first information on the full length sequence of the *NKCC* derived from the gills of

S. paramamosain (Fig. 1). Phylogenetic analysis of the SpNKCC confirmed its similarity to crustacean NKCC (Fig. 3). We know from previous studies that vertebrates NKCC duplicated in two major isoforms: a basolateral isoform (NKCC1), involved in NaCl excretion and an apical form (NKCC2), involved in NaCl uptake (Markadieu and Delpire, 2014). However, the resulting sequence information was insufficient to classify the product as apical or basolateral. Whether a second NKCC isoform exists in the crustacean genome as it found in vertebrates warrants further investigation.

Structurally, the deduced SpNKCC contains all signature domains of the Na⁺-dependent subgroup of solute carrier 12 (SLC12) family of transporters, including a SLC12A domain, 12 transmembrane domains, intracellular N- and C-termini domain (Fig. 1) that is important for maturation, dimerization, and protein trafficking to the plasma membrane (Markadieu and Delpire, 2014). Previous studies have shown that NKCCs may be activated by direct phosphorylation in the NH₂-terminus during osmotic stress (Lytle and Forbush, 1992; Giménez and Forbush, 2005). The presence of numerous potential phosphorylation sites in the NH₂-terminus of the *S. paramamosain* might be involved in the up-regulation of NKCC. All NKCCs are glycoproteins (Lytle and Forbush, 1992; Arroyo et al., 2013) which possess sites for N-linked glycosylation within a large hydrophilic loop between putative TM7 and TM8 (Payne and Forbush, 1995), and the consensus sites for N-linked glycosylation had been identified in the NKCC of *S. paramamosain*. The glycosylation in the large TM7-TM8 loop was considered crucial for transport activity, membrane expression, and affinity for loop diuretics (Paredes et al., 2006).

The profile of *SpNKCC* expression in tissues showed that the *SpNKCC* transcript was highest in the posterior gills with a broad lower level expression of this transporter across many tissues (Fig. 4). The posterior gills of euryhaline crabs are believed to be particularly specialized for ion transport on the basis of high expression of the ion transport protein (Towle et al., 1997a). Given the direct correspondence between posterior gills and ion transport across multiple crustacean species, the expression of *SpNKCC* in the posterior gills may function as likely.

The gill ultrastructure of *S. paramamosain* verifies our interpretation of the



NKA α (A), *NHE* (B), *CAC* (C) and *AQP-1* (D) mRNA levels in posterior gills of *S. paramamosain* during the molt cycle. The molt stages are defined based on the established criteria (Drach and Tchernigovtzeff, 1967). Values are expressed as means \pm SEM, $n = 7$. Means with different superscript letters are significantly different (one-way ANOVA, Tukey's multiple comparisons test, $P < 0.05$).

regulatory mechanism of NKCC might exist in crustaceans. Future establishing the adequate NKCC antibody specific for decapod transporters could provide a useful tool to ascertain its physiological role in ion regulation.

Consistent with their roles in ions uptake, *NKA α* , *CAG*, *NHE* showed the similar pattern of gene expression as *SpNKCC* (Fig. 9). The dynamic changes in gene transcripts involved in branchial osmoregulation observed in the current experiment provide evidence that regulation of ions uptake in different molt stages involves a coordinated suite of changes in osmoregulatory genes. Adjusting levels of gene expression can be rapid in postmolt stages, with the largest degree of inductive scope occurring within the first 2–3 days after ecdysis, typically the same time period in which hemolymph osmotic and ionic concentrations stabilize at new, regular levels. The largest increase in *NKA α* and *CAC* expression was observed at postmolt stage following ecdysis in the gills of *S. paramamosain*, perhaps therefore providing driving force and enhancing the supply of counterions for NaCl uptake respectively as outlined above. Increased *NKA α* and *CAC* transcription would increase the pool of *NKA α* and *CAC* protein. For example, in the blue crab *C. sapidus*, elevated activity of *NKA* during postmolt was observed (Towle and Mangum, 1985). In parallel, *NHE*, has been considered as a candidate in the uptake of Na^+ by gills of euryhaline crabs living in low salinities (Towle and Weihrauch, 2001; McNamara and Faria, 2012). Although the localization of *NHE* have not yet been explored in crustacean gills, the higher expression levels of *NHE* in the posterior gills of *C. maenas* than that in the anterior gills may therefore indicate a role of this antiporter in osmoregulation as previously suggested for fish (Choe et al., 2005; Scott et al., 2005; Kumai and Perry, 2012). Moreover, a recent study in our lab have shown that the relative abundance of *NHE* mRNA in the posterior gills of *S. paramamosain* was increased significantly after transfer from 28 to 5 ppt (Xu et al., unpublished).

This suggests that *NHE* may play a role in NaCl uptake when crabs are resident in low salinity. In this study, the increased expression of *NHE* (10.5 to 79.9-fold) in the gills during the ion uptake stages may provide more compelling support for a role of *NHE* in Na^+/H^+ exchange during the postmolt stages.

The aquaporin (*AQP*) family of water channels, small and very hydrophobic intrinsic membrane proteins, has been identified to potentially play roles in water and solute transport (Borgnia et al., 1999). In marine fish, the *AQP-1* has been shown to be vital for absorption of imbibed water across the cell membrane by up-regulating its mRNA expression (Aoki et al., 2003; Martinez et al., 2005; Giffard-Mena et al., 2007; Raldúa et al., 2008). In contrast, the involvement of aquaporins in water transport has been rarely studied in crustacean. Gao et al. (2009) demonstrated the relative mRNA expression of *AQP* in antennal gland was lower in the premolt when compared to the intermolt and postmolt stages. Additionally, the *AQP-1* expression of *C. sapidus* differed with ontogeny during larval development, with significantly higher expression at early larval stages in the exposure of hyposalinity (Chung et al., 2012). In this study, the expression of *AQP-1* in the posterior gills was significantly increased from molting to postmolt (Fig. 9D). Given the visible changes in uptake of water around ecdysis and elimination of water load in postmolt, the higher expression of *AQP-1* in gills of *S. paramamosain* may be responsible for water absorption at molting to aid in the exuviation process.

In summary, the present study identified a full length ortholog of the $\text{Na}^+/\text{K}^+/\text{2Cl}^-$ cotransporter, *SpNKCC*, in *S. paramamosain*. The *SpNKCC* transcript was abundantly expressed in ion-regulating gills. Expression of *SpNKCC* and a coordinated suite of genes increased in gills of *S. paramamosain* in the postmolt stages when ion uptake rate was demonstrated to increase significantly. This suggests that *SpNKCC* may

implicate its involvement in the ion uptake of *S. paramamosain* in the postmolt stages.

Supplementary data to this article can be found online at <http://dx.doi.org/10.1016/j.cbpa.2016.08.019>.



This work was funded by Zhejiang Provincial Key Project of Science and Technology Research (No. 2015C02054), Zhejiang Provincial Key Project of Aquaculture Breeding (No. 2016).

- Aoki, M., Kaneko, T., Katoh, F., Hasegawa, S., Tsutsui, N., Aida, K., 2003. Intestinal water absorption through aquaporin 1 expressed in the apical membrane of mucosal epithelial cells in seawater-adapted Japanese eel. *J. Exp. Biol.* 206, 3495–3505.
- Arroyo, J.P., Kahle, K.T., Gamba, G., 2013. The SLC12 family of electroneutral cation-coupled chloride cotransporters. *Mol. Asp. Med.* 34, 288–298.
- Borgnia, M., Nielsen, S., Engel, A., Agre, P., 1999. Cellular and molecular biology of the aquaporin. *Annu. Rev. Biochem.* 68, 425–458.
- Boudour-Boucheher, N., Boulo, V., Charmantier-Daures, M., Grousset, E., Anger, K., Charmantier, G., Lorin-Nebel, C., 2014. Differential distribution of V-type H⁺-ATPase and Na⁺/K⁺-ATPase in the branchial chamber of the palaemonid shrimp *Macrobrachium amazonicum*. *Cell Tissue Res.* 357, 195–206.
- Chang, Y.J., Sun, C.L., Chen, Y., Yeh, S.Z., 2011. Modelling the growth of crustacean species. *Rev. Fish Biol. Fish.* 22, 157–187.
- Choe, K.P., Kato, A., Hirose, S., Plata, C., Sindic, A., Romero, M.F., Claiborne, J.B., Evans, D.H., 2005. NH3 in an ancestral vertebrate: primary sequence, distribution, localization, and function in gills. *Am. J. Physiol. Regul. Integr. Comp. Physiol.* 289, 1520–1534.
- Chung, K.F., Lin, H.C., 2006. Osmoregulation and Na⁺/K⁺-ATPase expression in osmoregulatory organs of *Scylla paramamosain*. *Biochem. Physiol. A* 144, 48–57.
- Chung, J.S., Maurer, L., Bratcher, M., 2012. Cloning of aquaporin-1 of the blue crab, *Callinectes sapidus*: its expression during the larval development in hyposalinity. *Aquat. Biosyst.* 8, 21.
- Drach, P., Tchernigovtzeff, C., 1967. Sur la méthode de détermination des stades d'intermue et son application générale aux crustacés (in French with English abstract). *Vie Milieu Ser. A* 18, 595–609.
- Freire, C.A., Onken, H., McNamara, J.C., 2008. A structure-function analysis of ion transport in crustacean gills and excretory organs. *Biochem. Physiol. A* 151, 272–304.
- Gagnon, E., Forbush, B., Caron, L., Isemering, P., 2002. Functional comparison of renal Na⁺/K⁺/2Cl⁻ cotransporters between distant species. *Am. J. Physiol. Cell Physiol.* 284, 365–370.
- Gamba, G., 2005. Molecular physiology and pathophysiology of electroneutral cation-chloride cotransporters. *Physiol. Rev.* 85, 423–493.
- Gao, Y., Gao, Y.P., Wheatly, M., Krane, C., 2009. Cloning and expression of aquaporin in the antennal gland of crayfish, *Procambarus clarkii*. *FASEB J.* 23, 998.6.
- Ghanawi, J., Saoud, I.P., 2012. Molting, reproductive biology, and hatchery management of redclaw crayfish *Cherax quadricarinatus* (von Martens 1868). *Aquaculture* 358, 183–195.
- Giffard-Mena, I., Boulo, V., Aujoulat, F., Fowden, H., Castille, R., Charmantier, G., Cramb, G., 2007. Aquaporin molecular characterization in the sea-bass (*Dicentrarchus labrax*): the effect of salinity on AQP-1 and AQP-3 expression. *Comp. Biochem. Physiol. A Mol. Integr. Physiol.* 148, 430–444.
- Giménez, I., Forbush, B., 2005. Regulatory phosphorylation sites in the NH₂ terminus of the renal Na⁺/K⁺/2Cl⁻ cotransporter (NKCC2). *Am. J. Physiol. Ren. Physiol.* 289, 1341–1345.
- Goodman, S.H., Cavey, M.J., 1990. Organization of a phyllobranchiate gill from the green shore crab *Carcinus maenas* (Crustacea, Decapoda). *Cell Tissue Res.* 260, 495–505.
- Havird, J.C., Santos, S.R., Henry, R.P., 2014. Osmoregulation in the Hawaiian anchialine shrimp *Halocaridina rubra* (Crustacea: Atyidae): expression of ion transporters, mitochondria-rich cell proliferation and hemolymph osmolality during salinity transfers. *J. Exp. Biol.* 217, 2309–2320.
- Henry, R.P., 1988. Multiple functions of gill carbonic anhydrase. *J. Exp. Zool.* 248, 19–24.
- Huang, J.R., Huang, H.Y., Ye, H.H., 2012. Cloning and analysis of beta-actin gene from *Scylla paramamosain*. *J. Xiamen Univ.* 51, 274–279 (in Chinese with English abstract).
- Jasmani, S., Jayasankar, V., Shinji, J., Wilder, M.N., 2010. Carbonic anhydrase and Na⁺/K⁺-ATPase activities during the molt cycle of low salinity-reared white shrimp *Litopenaeus vannamei*. *Fish. Sci.* 76, 219–225.
- Kumai, Y., Perry, S.F., 2012. Mechanisms and regulation of Na⁺ uptake by freshwater fish. *Respir. Physiol. Neurobiol.* 184, 249–256.
- Leone, F.A., Garçon, D.P., Lucena, M.N., Faleiros, R.O., Azevedo, S.V., Pinto, M.R., McNamara, J.C., 2015. Gill-specific Na⁺/K⁺-ATPase activity and α -subunit mRNA expression during low-salinity acclimation of the ornate blue crab *Callinectes ornatus* (Decapoda, Brachyura). *Comp. Biochem. Physiol. B* 186, 59–67.
- Li, X., Xu, Z., Zhou, G., Lin, H., Zhou, J., Zeng, Q., Mao, Z., Gu, X., 2015. Molecular characterization and expression analysis of five chitinases associated with molting in the Chinese mitten crab, *Eriocheir sinensis*. *Biochem. Physiol. B* 187, 110–120.
- Livak, K.J., Schmittgen, T.D., 2001. Analysis of relative gene expression data using real-time quantitative PCR and the 2(T)(-Delta Delta C) method. *Methods* 25, 402–408.
- Luquet, C.M., Weihrauch, D., Senek, M., Towle, D.W., 2005. Induction of branchial ion transporter mRNA expression during acclimation to salinity change in the euryhaline crab *Chasmagnathus granulatus*. *J. Exp. Biol.* 208, 3627–3636.
- Lytle, C., Forbush, B., 1992. The Na⁺/K⁺/2Cl⁻ cotransporter protein of shark rectal gland. 2. Regulation by direct phosphorylation. *J. Biol. Chem.* 267, 25438–25443.
- Markadieu, N., Delpire, E., 2014. Physiology and pathophysiology of SLC12A1/2 transporters. *Pflugers Arch. - Eur. J. Physiol.* 466, 91–105.
- Martinez, A.S., Cutler, C.P., Wilson, G.D., Phillips, C., Hazon, N., Cramb, G., 2005. Cloning and expression of three aquaporin homologues from the European eel (*Anguilla anguilla*): effects of seawater acclimation and cortisol treatment on renal expression. *Biol. Cell.* 97, 615–627.
- McNamara, J.C., Faria, S.C., 2012. Evolution of osmoregulatory patterns and gill ion transport mechanisms in the decapod Crustacea: a review. *J. Comp. Physiol. B* 182, 997–1014.
- Ong, K.S., 1966. Observations on the post-larval life history of *Scylla serrata* reared in the laboratory. *Malays. Agric. J.* 45, 429–445.
- Paredes, A., Plata, C., Rivera, M., Moreno, E., Vazquez, N., Munoz-Clares, R., Hebert, S.C., Gamba, G., 2006. Activity of the renal Na⁺/K⁺/2Cl⁻ cotransporter is reduced by mutagenesis of N-glycosylation sites: role for protein surface charge in Cl⁻ transport. *Am. J. Physiol. Ren. Physiol.* 290, 1094–1102.
- Payne, J.A., Forbush, B., 1995. Molecular characterization of the epithelial Na⁺/K⁺/2Cl⁻ cotransporter isoforms. *Curr. Opin. Cell Biol.* 7, 493–503.
- Perry, H., Trigg, C., Larsen, K., Freeman, J., Erickson, M., Henry, R., 2001. Calcium concentration in seawater and exoskeletal calcification in the blue crab, *Callinectes sapidus*. *Aquaculture* 198, 197–208.
- Raldúa, D., Otero, D., Fabra, M., Cerdá, J., 2008. Differential localization and regulation of two aquaporin-1 homologs in the intestinal epithelia of the marine teleost *Sparus aurata*. *Am. J. Physiol. Regul. Integr. Comp. Physiol.* 294, 993–1003.
- Riestenpatt, S., Onken, H., Siebers, D., 1996. Active absorption of Na⁺ and Cl⁻ across the gill epithelium of the shore crab *Carcinus maenas*: voltage-clamp and ion-flux studies. *J. Exp. Biol.* 199, 1545–1554.
- Robertson, J.D., 1960. Osmotic and ionic regulation. In: Waterman, T.H. (Ed.), *The Physiology of Crustaceans* vol. 1. Academic Press, New York, pp. 317–339.
- Scott, G.R., Claiborne, J.B., Edwards, S.L., Schulte, P.M., Wood, C.M., 2005. Gene expression after freshwater transfer in gills and opercular epithelia of killifish: insight into divergent mechanisms of ion transport. *J. Exp. Biol.* 208, 2719–2729.
- Serrano, L., Henry, R.P., 2008. Differential expression and induction of two carbonic anhydrase isoforms in the gills of the euryhaline green crab, *Carcinus maenas*, in response to low salinity. *Biochem. Physiol. D* 3, 186–193.
- Serrano, L., Halanych, K.M., Henry, R.P., 2007. Salinity-stimulated changes in expression and activity of two carbonic anhydrase isoforms in the blue crab *Callinectes sapidus*. *J. Exp. Biol.* 210, 2320–2332.
- Spanings-Pierrot, C., Towle, D.W., 2004. Salinity-related mRNA expression of the Na⁺/K⁺/2Cl⁻ cotransporter and V-type H⁺-ATPase in gills of the euryhaline crab *Pachygrapsus marmoratus*. *Bull. Mt. Desert Isl. Biol. Lab.* 43, 6–8.
- Tamura, K., Peterson, D., Peterson, N., Stecher, G., Nei, M., Kumar, S., 2011. MEGA5: molecular evolutionary genetics analysis using maximum likelihood, evolutionary distance, and maximum parsimony methods. *Mol. Biol. Evol.* 28, 2731–2739.
- Towle, D.W., Mangum, C.P., 1985. Ionic regulation and transport ATPase activities during the molt cycle in the blue crab *Callinectes sapidus*. *J. Crustac. Biol.* 5, 216–222.
- Towle, D.W., Weihrauch, D., 2001. Osmoregulation by gills of euryhaline crabs: molecular analysis of transporters. *Am. Zool.* 41, 770–780.
- Towle, D.W., Rushton, M.E., Heidysch, D., Magnani, J.J., Rose, M.J., Amstutz, A., Jordan, M.K., Shearer, D.W., Wu, W.S., 1997a. Sodium/proton antiporter in the euryhaline crab *Carcinus maenas*: molecular cloning, expression and tissue distribution. *J. Exp. Biol.* 200, 1003–1014.
- Towle, D.W., Weihrauch, D., Fooks, A., Cohen, Z.S., 1997b. Molecular identification and cDNA sequencing of a Na⁺/K⁺/2Cl⁻ cotransporter in gills of the euryhaline blue crab *Callinectes sapidus*. *Am. Zool.* 37, 87A.
- Wilder, M.N., Huang, D.T.T., Jasmani, S., Jayasankar, V., Kaneko, T., Aida, K., Hatta, T., Nemoto, S., Wigginton, A., 2009. Hemolymph osmolality, ion concentrations and calcium in the structural organization of the cuticle of the giant freshwater prawn *Macrobrachium rosenbergii*: changes with the molt cycle. *Aquaculture* 292, 104–110.
- Xu, B.P., Tu, D.D., Shu, M.A., 2016. Identification and expression of an Na⁺/H⁺ exchanger (NHE) in the gills of the euryhaline mud crab, *Scylla paramamosain*, in response to low salinity seawater, unpublished.
- Xu, B.P., Long, C., Dong, W.R., Shao, Q.J., Shu, M.A., 2015. Molecular characterization of calreticulin gene in mud crab *Scylla paramamosain*: implications for the regulation of calcium homeostasis during molt cycle. *Aquac. Res.* <http://dx.doi.org/10.1111/are.12781>.